ORIGINAL SCIENTIFIC PAPER

Lib Oncol. 2022;50(2-3):52–61

doi: 10.20471/LO.2022.50.02-03.10

HYDROGEN BONDS ENERGY DISTRIBUTION AND INFORMATION-THEORETIC ANALYSIS OF BLOOD SERUM FROM HAMSTERS WITH EXPERIMENTAL *GRAFFI* TUMOR

NIKOLAI NESHEV[1], IGNAT IGNATOV[2], RENETA TOSHKOVA[3], CRISTOS DROSSINAKIS[4] and GEORGI GLUHCHEV[5]

[1]Faculty of Physics, Sofia University *St. Kliment Ohridski*, Sofia, Bulgaria;
[2]Scientific Research Center of Medical Biophysics (SRCMB), Sofia, Bulgaria;
[3]Institute of Experimental Morphology, Pathology and Anthropology with Museum, Bulgarian Academy of Sciences, Sofia, Bulgaria;
[4]IAWG - Internationale Akademie für Wissenschaftliche Geistheilung, Frankfurt, Germany;
[5]Institute of Information and Communication Technologies, Bulgarian Academy of Science (BAS), Sofia, Bulgaria

Summary

The aim of the present study was to estimate the feasibility of blood serum hydrogen bonds energy distribution, and information-theoretic characteristics, as diagnostic markers for tumor disease in *Graffi* tumor bearing hamsters. *Golden Syrian* hamsters were randomly divided into two groups: a healthy control and an experimental one, challenged with *Graffi* tumor cells. The distributions of hydrogen bonds energies (-E) in the blood serum samples were investigated with a non-equilibrium process of droplets evaporation and sequential measurements of their wetting angle (Non-equilibrium Energy Spectrum (NES)). The measurements show significantly lower average hydrogen bond energy of the experimental samples than the controls. Shifts in NES toward depletion of (-E) at energy levels 0.0937, 0.1187, 0.1212, 0.1337, and 0.1387 eV, and an additional population at 0.0987, 0.1012, 0.1137, and 0.1237 eV energy levels were observed in the experimental samples compared to the controls. Such a pattern points to the possibility of utilizing the *f*(E) shifts at these energy levels as diagnostic markers of *Graffi* tumor in hamsters. Information-theoretic measures of Shannon entropy, Variation of information and Transformational information entropy were used to investigate possible differences between the experimental and control spectrum. Although they differ significantly in definitions, a comparison with the three information-theoretic measures did not reveal a statistically significant difference.

KEYWORDS: *hydrogen bonds, energy, information, entropy, blood serum, tumor*

INTRODUCTION

Long-term efforts have been dedicated to investigations of blood serum as a possible source of cancer diagnostics information. Rai et al.(1) focused their work on oral submucous fibrosis (OSF) due to its highest malignant potentiality compared to all other pre-cancerous lesions and the difficulty of its clinical detection prior to invasive and painful tissue biopsy. They used Fourier transform infrared (FTIR) spectroscopy combined with chemometric techniques to compare the serum metabolic signatures of OSF patients and healthy controls. The FTIR findings were further supported by serum biochemical analyses. As a result, absorbance intensities of 45 infrared wavenumbers were found to be significantly different in OSF and normal serum

***Corresponding author**: Ignat Ignatov, Faculty of Physics, Sofia University St. Kliment Ohridski, Sofia 1000, Bulgaria. E-mail: mbioph@abv.bg*

FTIR spectra corresponding to alterations in carbohydrates, proteins, lipids and nucleic acids. Nineteen prominent significant wavenumbers ($P \leq 0.001$) at 1020, 1025, 1035, 1039, 1045, 1078, 1055, 1100, 1117, 1122, 1151, 1169, 1243, 1313, 1398, 1453, 1544, 1650 and 1725 cm^{-1} allowed for effective discrimination between OSF and normal spectra by using multivariate statistical techniques. The authors concluded that metabolic features of blood serum of OSF patients analysed with FTIR spectroscopy coupled with chemometric analysis can be potentially useful for rapid and accurate preoperative screening/diagnosis of OSF.

Duo et al.(2) used gold nanoparticle-based surface-enhanced Raman spectroscopy (SERS) to investigate blood serum biochemical characteristics for non-invasive colorectal cancer detection. SERS measurements were performed on a group of patients with pathologically confirmed colorectal cancer and on another group of healthy volunteers (control subjects). The assigned Raman bands in the measured SERS spectra displayed cancer specific biomolecular changes, including an increase in the relative amounts of nucleic acid, a decrease in the percentage of saccharide and proteins contents in the blood serum of colorectal cancer patients as compared to healthy subjects. A combination of empirical approach and multivariate statistical techniques, including principal components analysis (PCA) and linear discriminant analysis (LDA) was used for development of effective diagnostic algorithms for classification of SERS spectra between the normal and colorectal cancer serum. The empirical diagnostic algorithm, based on the ratio of the SERS peak intensity at 725 cm^{-1} for adenine to the peak intensity at 638 cm^{-1} for tyrosine, achieved a diagnostic sensitivity of 68.4% and specificity of 95.6%, while diagnostic algorithms based on PCA-LDA had a diagnostic sensitivity of 97.4% and specificity of 100% for separating cancerous samples from normal samples. These results demonstrated that gold nanoparticle-based SERS serum analysis combined with PCA-LDA has significant potential for non-invasive detection of colorectal cancers.

Sitnikova et al.(3) proposed infrared spectroscopy of a blood serum as an accessible and quick method for breast cancer detection. In particular, authors used multivariate processing of IR spectra of a human blood serum obtained by attenuated total reflectance Fourier transform infrared (ATR-FTIR) spectroscopy. They examined blood samples from 66 patients who had been clinically diagnosed with breast cancer, and from 80 healthy volunteers. Their combined approach was based on a principal component analysis (PCA) and a principal component regression (PCR). The PCA method allowed for determination of the spectral bands connected with the intensity differences between the control group and the patient group. As a result, the IR spectrum of a blood serum was shown to be diagnostically significant for breast cancer by corresponding to the vibrations of several functional groups of DNA and RNA. The obtained values of sensitivity (92.3%) and specificity (87.1%) were close to those of mammography and ultrasound, thus pointing to the feasibility of this method for real clinical laboratory diagnostics.

Yue et al.(4) worked on laser-induced breakdown spectroscopy (LIBS) for detection of an ovarian cancer fingerprint in a human blood plasma. They developed machine learning data analysis combining feature selection and regression with a back-propagation neural network. Their classification models for cancer detection were applied on 176 blood plasma samples collected from ovarian cyst patients and normal cases. Cancer diagnosis sensitivity of 71.4% and specificity of 86.5% were obtained for randomly selected validation samples.

Nahon et al.(5), using a multiparametric analysis technique, assessed the metabolomic profiles of a serum, obtained by the proton nuclear magnetic resonance (NMR) spectroscopy, from cirrhotic patients with and without hepatocellular carcinoma (HCC). The study included 154 patients with compensated biopsy-proven alcoholic cirrhosis. Proton spectra were measured at 500 MHz. The authors developed an orthogonal partial latent structure [orthogonal projection to latent structure (OPLS)] analysis model to discriminate large HCC spectra from cirrhotic spectra. Small HCC spectra were secondarily projected using previously built OPLS discriminant components. As a result, the OPLS model was shown to discriminate between cirrhotic and large HCC spectra. Glutamate, acetate, and N-acetyl glycoproteins significantly increased with large HCC whereas lipids and glutamine correlated with cirrhosis. A heterogeneous distribution between large HCC and cirrhotic samples was shown by

projection of small HCC samples into the OPLS model. During follow-up, the small HCC patients with metabolomic profile similar to those in the large HCC group had higher incidences of the recurrence or death. It was concluded that the serum NMR-based metabolomics was able to identify metabolic fingerprints that could be specific to the large HCC in cirrhotic livers. In addition, some patients with small HCC eligible for curative treatments were qualified by OPLS model as similar to patients with advanced cancerous disease. Although the authors recommended further investigations of these patients to clearly define the subgroup with a worse prognosis, it was clear that the NMR spectra of the blood serum could possibly be applied for a detection of an early-stage cancer.

To further expand the range of such possibilities, the aim of the present study was to estimate the feasibility of the blood serum hydrogen bonds energy distribution and information- theoretic characteristics as diagnostic markers for tumor disease in *Graffi* tumor bearing hamsters.

MATERIALS AND METHODS

Animals

Golden Syrian hamsters (male and female), aged 2-4 months, weighing approx. 100 g purchased from Slivnitza experimental and breeding base for laboratory animals at Bulgarian Academy of Sciences were used. All animals were acclimatized to the laboratory environment for a week before the experiment. Hamsters were individually housed in plastic cages in a temperature-controlled room (25±2^{0}C), with 12h light/dark cycle. They were provided with free access to rodent chow and water ad libitum. Experiments were carried out in the Institute of Experimental Morphology, Pathology and Anthropology with Museum, Bulgarian Academy of Sciences (IEMPAM-BAS) (Permission No. 11 30 127) in accordance with the national regulation No. 20/01.11.2012 regarding laboratory animals and animal welfare, European directive 2010/63/EU of the European Parliament, and of the Council of 22 September 2010 on the protection of animals used for scientific purposes.

Experimental design

The hamster *Graffi* tumor model was established and maintained at IEMPAM-BAS by Toshkova(6). *Graffi* myeloid tumor is a transplantable, fast-growing solid tumor adapted and equally developing in hamsters of both sexes. It is characterized by 100% transplantability, 100% mortality and absence of spontaneous regression. Seven to fifteen days after subcutaneous injection of *Graffi* tumor cells, tumor appears as a palpable nodule under the skin at the injection site, which progressively grows to a size of about 40 mm and causes death in the experimental animals. This experimental tumor is a reliable model for drug screening and cancer-related research. It has been applied in research of chemical compounds as glycosylated Cu/Zn-containing superoxide dismutase(7), phenanthroline derivatives(8)**;** medicinal plants as Astragalus glycypphyllos(9), algae as Porphyridium cruentum(10); food additives as chitosan(11), Cortinon(12); catholyte water from the process of electrolysis with negative redox potential ORP=-400±4 mV and pH=9.5±0.11(13).

The hamsters were randomly divided into two groups of 9 according to our experimental protocol: the control group consisted of healthy animals without tumors (C), and the experimental group consisted of hamsters challenged with the *Graffi* tumor cells (TBH). The distribution by sex in both groups was not taken into account because of the above-mentioned specifics of the *Graffi* tumor model. In brief, a tumor cell suspension for animal inoculation was prepared by mincing tumor fragments with scissors on an 80-mesh nylon screen. Tumor cells were washed in PBS through centrifugation (500 g for 5 min, 4^{0}C), and a dose of 500 μL containing 1.10^4 cells was given subcutaneously (s.c.) into the interscapular region of the recipient hamsters. The tumor size was measured with palpation and signs of appearance were evident in7 to 15 days after inoculation.

The experimental and control hamsters were sacrificed by cervical dislocation, after the etherisation, 15 days after tumor inoculation. The blood was collected directly by dripping into the preservative-free tubes (the stopper of the tube was removed preliminary), then allowed it to clot by leaving for 20–30 minutes at the room temperature (23^{0}C) and then cooled on ice. Serum was separated by centrifugation at 1000–2000 x g for 10 minutes in a refrigerated centrifuge. The resulting serum was immediately transferred into a clean polypropylene tube using a Pasteur pipette. The

samples were apportioned into 0.5 ml aliquots and were maintained at 2-8^{0}C prior analysis.

Measurements of Non-equilibrium Energy Spectra

The distributions of hydrogen bonds energies in the blood serum samples were investigated with a method invented by Antonov, based on the non-equilibrium process of droplets evaporation and sequential measurements of their wetting angle(14-16). Thus, the non-equilibrium energy spectrum (NES) was determined as a function f(E) where the energy E is expressed in eV. Water droplets, 10 of each sample, evaporated on a thin biaxially-oriented polyethylene terephthalate (BoPET) foil over a glass plate in the hermetic chamber.

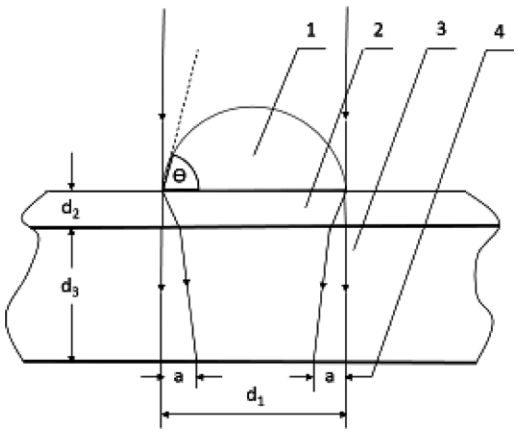

*Fig. 1. Measurement of the wetting angle of liquids:1-drop, 2 – thin BoPET foil, 3 –glass plate, 4 – refraction ring width (**a**). The wetting angle θ is calculated by using the measured values of **a**, and $\boldsymbol{d}_3$ (the thickness of the glass plate). The thickness of the BoPET foil is $\boldsymbol{d}_2$ and the diameter of the refraction ring is $\boldsymbol{d}_1$.*

The experimental setup is shown in Figure 1. Parallel beams of monochromatic light with 580±7 nm wavelength were radiated normally to the BoPET foil and the glass plate. The device allowed for the measurements of wetting angles in a range from 72.3 to 0 deg, corresponding to the hydrogen bonds energy in a range of E from -0.08 to -0.1387 eV. The temperature in the hermetic chamber was 23±1^{0}C.

During evaporation, for approx. 3 hours, the wetting angles of all droplets were measured sequentially in the 10 min intervals, and the average distributions of wetting angles f(θ) were calculated.

Subsequently, the normalized distributions of the hydrogen bonds energies f(E) were calculated as:

$$f(E) = \frac{14{,}33\, f(\theta)}{[1-(1+bE)^2]^2} \qquad (1)$$

where E is a hydrogen bonds energy expressed in eV. Because it is defined as binding energy and its values are originally negative, all tables and graphs below show the values of –E for simplicity. The NES of each sample was determined as the average NES of the 10 simultaneously measured droplets from it. The average energy of hydrogen bonds was also calculated as follows:

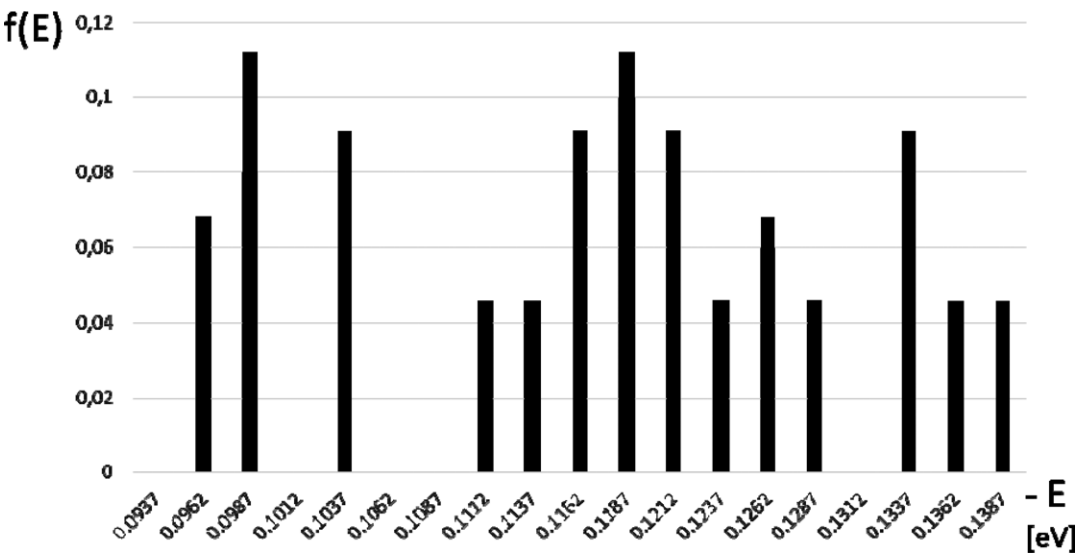

Fig. 2. NES of deionized water

Table 1.

NES of the experimental blood serum samples

Experimental Sample No. / Energy (-E) [eV]	1	2	3	4	5	6	7	8	9
0.0937	0.000	0.000	0.000	0.000	0.000	0.000	0.000	0.000	0.000
0.0962	0.000	0.091	0.160	0.000	0.000	0.105	0.043	0.045	0.043
0.0987	0.125	0.135	0.084	0.111	0.086	0.105	0.087	0.045	0.087
0.1012	0.125	0.135	0.084	0.000	0.086	0.105	0.087	0.065	0.043
0.1037	0.000	0.091	0.000	0.111	0.051	0.000	0.043	0.076	0.087
0.1062	0.125	0.000	0.084	0.111	0.051	0.105	0.087	0.091	0.087
0.1087	0.000	0.000	0.000	0.111	0.086	0.000	0.000	0.045	0.000
0.1112	0.125	0.091	0.042	0.000	0.086	0.000	0.087	0.045	0.087
0.1137	0.125	0.091	0.042	0.000	0.051	0.105	0.087	0.091	0.087
0.1162	0.000	0.000	0.000	0.055	0.051	0.105	0.043	0.045	0.000
0.1187	0.000	0.000	0.084	0.000	0.000	0.000	0.043	0.045	0.043
0.1212	0.000	0.091	0.084	0.111	0.051	0.105	0.043	0.045	0.087
0.1237	0.125	0.000	0.084	0.111	0.086	0.105	0.087	0.091	0.087
0.1262	0.125	0.000	0.084	0.111	0.051	0.000	0.091	0.091	0.087
0.1287	0.000	0.091	0.000	0.000	0.086	0.000	0.043	0.000	0.043
0.1312	0.000	0.046	0.084	0.056	0.000	0.000	0.043	0.045	0.043
0.1337	0.000	0.046	0.042	0.000	0.086	0.000	0.043	0.045	0.000
0.1362	0.063	0.046	0.042	0.056	0.093	0.055	0.043	0.045	0.089
0.1387	0.062	0.046	0.000	0.056	0.000	0.105	0.000	0.045	0.000

$$< E > = \sum f(E_i).E_i \quad (2)$$

by using all the corresponding discrete values.

Information-theoretic analysis

As non-equilibrium energy spectra represent probabilistic distributions of hydrogen bond energies (17,18), three different information-theoretic measures were used for investigation of possible differences of these measures(19,20) between the spectra of blood serum samples.

The *Shannon entropy* (H) of a probability distribution (P) is defined as (21):

$$H(P) = -\sum_{i=1}^{n} p_i \log(p_i) \quad (3)$$

where n is the number of possible outcomes and p_i is the probability of the i-th outcome. In the present work, base 2 logarithm was used, so Shannon entropy was calculated in bits. It has been the first and most popular measure of information content applied extensively in analyses of differences between processes or states in a great variety of systems. So, having in mind the complex shapes of NES, it was expected to characterize the variable prevalence of hydrogen bonds energy values in the blood serum samples caused by tumor development.

In addition, the measures of *variation of information* (VI) and *transformational information entropy* (TI) (19,20) were used to determine the information differences between the NES of blood serum samples and deionized water as a standard solvent. These alternatives are feasible for the possibility to compare hydrogen bonds energy distributions in the natural structure of deionized water with those in the blood serum samples altered by dissolved substances and biochemical processes.

The *variation of information* (VI) is a measure of the distance between two partitions of elements(22).

Table 2.

NES of the control blood serum samples

Control Sample No. / Energy [No.]	1	2	3	4	5	6	7	8	9
0.0937	0.000	0.081	0.000	0.042	0.000	0.051	0.037	0.000	0.032
0.0962	0.000	0.081	0.095	0.000	0.051	0.026	0.074	0.038	0.064
0.0987	0.043	0.000	0.095	0.000	0.051	0.039	0.000	0.038	0.032
0.1012	0.043	0.000	0.000	0.084	0.058	0.039	0.055	0.038	0.048
0.1037	0.092	0.081	0.095	0.113	0.038	0.051	0.000	0.093	0.048
0.1062	0.092	0.109	0.048	0.000	0.058	0.026	0.037	0.000	0.032
0.1087	0.043	0.045	0.000	0.000	0.038	0.051	0.037	0.062	0.032
0.1112	0.000	0.109	0.048	0.000	0.051	0.051	0.074	0.062	0.064
0.1137	0.000	0.000	0.000	0.042	0.051	0.026	0.000	0.000	0.032
0.1162	0.092	0.000	0.000	0.084	0.038	0.026	0.037	0.062	0.032
0.1187	0.092	0.081	0.048	0.042	0.058	0.051	0.074	0.062	0.064
0.1212	0.135	0.161	0.285	0.115	0.119	0.207	0.168	0.135	0.135
0.1237	0.000	0.045	0.000	0.000	0.038	0.026	0.037	0.038	0.032
0.1262	0.092	0.000	0.000	0.042	0.038	0.026	0.037	0.062	0.064
0.1287	0.000	0.000	0.000	0.084	0.058	0.051	0.037	0.000	0.032
0.1312	0.000	0.081	0.095	0.042	0.083	0.078	0.074	0.062	0.048
0.1337	0.092	0.000	0.048	0.113	0.058	0.051	0.055	0.093	0.048
0.1362	0.092	0.045	0.048	0.084	0.058	0.078	0.055	0.062	0.064
0.1387	0.092	0.081	0.095	0.113	0.058	0.051	0.112	0.093	0.097

If X = $\{X_1, X_2,\ldots,X_k\}$ and Y= $\{Y_1,Y_2,\ldots,Y_k\}$ are two partitions of a set C into disjoint subsets, let:

$$n = \sum_i |X_i| = \sum_j |Y_j| = |C|$$

$$p_i = \frac{|X_i|}{n} q_j = \frac{|Y_j|}{n}$$

$$r_{ij} = \frac{|X_i \cap Y_j|}{n}$$

Then, the variation of information (VI) between the two partitions is defined as:

$$VI(X;Y) = -\sum_{i,j}^{n} r_{ij}\left[\log\left(r_{ij}/p_i\right) + \log\left(r_{ij}/q_j\right)\right] \quad (4)$$

Transformational information entropy (TI) represents the amount of information necessary to transform the NES of deionized water into the NES of the investigated samples (19, 20).

If p and q are probability distributions on a finite set X, then:

$$TI(p,q) = \sum_{i \in X} |p_i \log(p_i) - q_i \log(q_i)| \quad (5)$$

Whenever p and/or q are zero, the contribution of the corresponding term is by definition zero because:

$$\lim_{y \to 0+}^{y\log(y)=0}$$

The NES of deionized water is shown in Figure 2.

Statistical Analysis

Statistical analysis of the NES, average energies and information-theoretical characteristics was performed with MATLAB software at 95% confidence level with the Mann-Whitney U test due to the experimental and control samples' deviation

Table 3.
Statistical comparison of experimental and control samples' NES

-E [eV]	Samples	Median	U	p-value	Hypothesis
0.0937	Exp.	0.000			
	C.	0.032	18	0.014	H_1
0.0962	Exp.	0.043			
	C.	0.051	40	1.000	H_0
0.0987	Exp.	0.087			
	C.	0.038	6	0.003	H_1
0.1012	Exp.	0.086			
	C.	0.043	14.5	0.024	H_1
0.1037	Exp.	0.051			
	C.	0.081	29.5	0.351	H_0
0.1062	Exp.	0.087			
	C.	0.037	20	0.07662	H_0
0.1087	Exp.	0.000			
	C.	0.038	30	0.356	H_0
0.1112	Exp.	0.086			
	C.	0.051	34	0.594	H_0
0.1137	Exp.	0.087			
	C.	0.000	9	0.005	H_1
0.1162	Exp.	0.043			
	C.	0.037	37	0.787	H_0
0.1187	Exp.	0.000			
	C.	0.062	11	0.010	H_1
0.1212	Exp.	0.084			
	C.	0.135	0	0.000	H_1
0.1237	Exp.	0.087			
	C.	0.032	7.5	0,004	H_1
0.1262	Exp.	0.087			
	C.	0.038	23	0.131	H_0
0.1287	Exp.	0.000			
	C.	0.032	40	1.000	H_0
0.1312	Exp.	0.043			
	C.	0.074	20.5	0.083	H_0
0.1337	Exp.	0.042			
	C.	0.055	12	0.012	H_1
01362	Exp.	0.055			
	C.	0.062	28	0.297	H_0
0.1387	Exp.	0.045			
	C.	0.093	10	0.008	H_1

from the normal distribution as well as because of their size. According to the established practice, the reported results include the medians of the compared samples (groups), the value of the calculated U statistics, the p-value and the acceptance (H_0) or rejection (H_1) of the null hypothesis.

RESULTS AND DISCUSSION

The NES of 9 experimental and 9 control blood serum samples are presented in Table 1 and Table 2.

The statistical comparison of the experimental and control samples' NES at each value of hydrogen bonds energy is shown in Table 3.

For overall visual representation, the medians of these NES are shown in Figure 3. The energies at which statistically significant differences were found are marked with an asterisk.

Here, distinct shifts were observed in the NES of the experimental samples towards depletion of (-E) with 0.0937 ($\tilde{\upsilon}$=756 cm^{-1}), 0.1187 (957), 0.1212 (978), 0.1337 (1078) and 0.1387 eV (1117) energy levels as well as extra population of the 0.0987 ($\tilde{\upsilon}$=796 cm^{-1}), 0.1012 (816), 0.1137 (937) and 0.1237 (998) eV energy levels. Such a pattern points to the possibility of utilizing the *f*(E) shifts at these energy levels as diagnostic markers of *Graffi* tumor in hamsters. Another implication of this finding is a possible tendency towards general decrease of hydrogen bonds energy in the blood serum due to the tumor. Along these lines, statistical analysis was performed on the average hydrogen bonds energy of the experimental and control samples calculated with their corresponding NES by using eq.(2). The results are shown in Table 4.

Values clearly demonstrate that the average hydrogen bonds energy of the experimental samples was lower than that of the control ones.

The median result of E=-0.1150 eV or $\tilde{\upsilon}$=928 cm^{-1} corresponds of the theoretical result of Gaussian distribution of clusters of water molecules or E=-0.1137 eV or $\tilde{\upsilon}$=917 cm^{-1}(23). That is why, such a shift in the average hydrogen bonds energy in blood serum can also be used as a diagnostic marker of *Graffi* tumor in hamsters. Moreover, together with the above-mentioned shifts in *f*(E), this approach could also be tested in other organisms bearing other kinds of tumors.

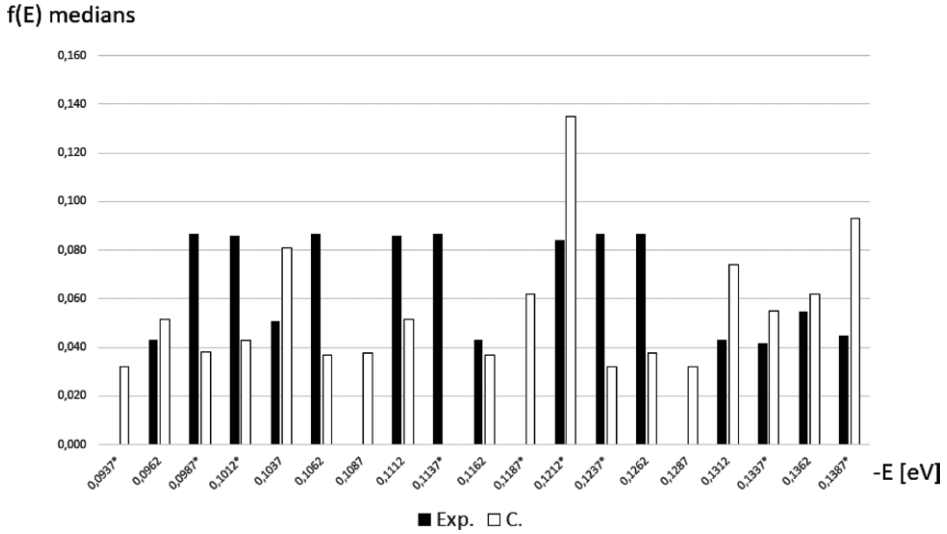

Figure 3. Medians of the experimental and control samples' NES at each value of hydrogen bonds energy. Statistically significant differences are marked with an asterisk.

Table 4.

Statistical comparison of the average hydrogen bonds energy of the experimental and control samples

SPL №	1	2	3	4	5	6	7	8	9				
Average Energy (-E) [eV]										**Median**	**U**	**p-value**	**Hyp.**
Exp.	0.1148	0.1132	0.1141	0.1166	0.1169	0.1140	0.1150	0.1161	0.1155	0.1150			
C.	0.1198	0.1151	0.1176	0.1215	0.1185	0.1187	0.1199	0.1199	0.1185	0.1187	4	0.00049	**H1**

Table 5.

Shannon entropy (H), transformational information entropy (TI) and variation of information (VI) of the experimental and control samples combined with statistical comparisons

SPL №	1	2	3	4	5	6	7	8	9				
H										**Median**	**U**	**p-value**	**Hyp.**
Exp.	3.13	3.49	3.59	3.39	3.76	3.30	3.91	4.01	3.74	3.59	28	0.30	H_0
C.	3.51	3.49	3.18	3.59	4.10	3.97	3.82	3.80	4.10	3.80			
TI													
Exp.	3.57	2.26	2.51	2.94	2.47	2.92	2.14	2.20	2.29	2.47			
C.	2.34	3.25	2.40	2.44	1.89	2.39	2.73	1.84	2.01	2.39	30	0.39	H_0
VI													
Exp.	0.25	0.24	0.29	0.23	0.37	0.27	0.47	0.43	0.33	0.29			
C.	0.26	0.24	0.37	0.33	0.42	0.55	0.38	0.34	0.45	0.37	26	0.22	H_0

According to previous works, the local maximum at E = -0.1212 eV; λ=10.23 μm; $\tilde{\upsilon}$=978 cm^{-1} is associated with anti-inflammatory effects while this at E=-0.1387 eV (λ=8.95 μm)($\tilde{\upsilon}$=1117 cm^{-1}) is associated with an inhibition of tumor cells development on a molecular level(24-27).

There were proofs of water molecules structuring at E=-0.1387 eV; λ=8.95 μm; $\tilde{\upsilon}$=1117 cm^{-1} in dodecahedra clusters with 20 water molecules of the size of 0.822 nm(28).

Same parameters at E=-0.1387 eV; λ=8.95 μm; $\tilde{\upsilon}$=1117 cm^{-1} are present in vibrations of a cluster of six water molecules(29).

The statistically significant differences in 9 out of 19 investigated hydrogen bonds energy levels lead to the question about the information content of NES and its relevance as a possible marker of *Graffi* tumor. In order to answer it, the information theoretical results for the Shannon entropy (H), transformational information entropy (TI)

and variation of information (VI) are presented in Table 5.

Although the three measures are substantially different in their definitions, no statistically significant differences were found between them for the experimental and control samples. Nevertheless, a fundamental question remains if these findings reflect some special feature of blood serum information content or further experiments on a larger scale might show statistically significant differences.

CONCLUSION

Investigation of the distributions of hydrogen bond energies in the blood serum of *Graffi* tumor bearing hamsters compared to a healthy ones showed statistically significant differences in the population of 9 out of 19 measured energy levels. In addition, the average hydrogen bonds energy of experimental (tumor bearing) samples was significantly lower compared to the control (healthy) ones. However, despite of substantial differences in terms of energy, three different information-theoretic measures, i.e. Shannon entropy, variation of information and transformational information entropy did not show statistical differences between the non-equilibrium energy spectra. Consequently, the distribution of hydrogen bonds energy could be used as a diagnostic marker for tumor disease in *Graffi* tumor bearing hamsters and possibly for cancer disease in general. The absence of statistically significant differences between the information-theoretic measures of all measured non-equilibrium energy spectra may be reflecting some unknown fundamental role of the blood in a biological regulation. This is why further work should help to elucidate this matter.

REFERENCES

1. Rai V, Mukherjee R, Routray A, Ghosh AK, Roy S, Barnali Ghosh P, et al. Serum-based diagnostic prediction of oral submucous fibrosis using FTIR spectrometry. Spectrochim. Acta A Mol Biomol Spectrosc. 2018;189: 322-329, doi: 10.1016/j.saa.2017.08.018.
2. Duo L, Shangyuan F, Jianji P, Yanping Ch, Juqiang J, Guannan Ch, et al. Colorectal cancer detection by gold nanoparticle based surface-enhanced Raman spectroscopy of blood serum and statistical analysis. Optics express. 2011;19:13565-13577, doi: 10.1364/OE.19.013565.
3. Sitnikova VE, Kotkova MA, Nosenko TN, Kotkova TN, Martynova DM, Uspenskaya MV. Breast cancer detection by ATR-FTIR spectroscopy of blood serum and multivariate data-analysis. Talanta. 2020;214: 120857, doi:10.1016/j.talanta.2020.120857.
4. Yue Z, Sun Ch, Chen F, Zhang Y, Xu W, Shabbir S, et al.. Machine learning-based LIBS spectrum analysis of human blood plasma allows ovarian cancer diagnosis. Biomed Opt Express. 2021;12:2559-74. doi:10.1364/BOE.421961.
5. Nahon P, Amathieu R, Triba MN, Bouchemal N, Nault JC, Ziol M, et al. Identification of serum proton NMR metabolomic fingerprints associated with hepatocellular carcinoma in patients with alcoholic cirrhosis. Clin Cancer Res. 2012;18(24):6714-22. doi: 10.1158/1078-0432.CCR-12-1099.
6. Toshkova R. Attemps for immunomodulation in hamsters with transplanted Myeloid tumor, previously induced by *Graffi* virus. Bulgarian Academy of Sciences, PhD thesis. Sofia. 2012.
7. Angelova M, Dolashka-Angelova P, Ivanova E, Serkedjieva J, Slokoska, Pasheova S, et al. A novel glycosylated Cu/Zn-containing superoxide dismutase: production and potential therapeutic effect, Microbiology. 2001;147(6), doi:10.1099/00221287-147-6-1641.
8. Wesselinova D, Neykov M, Kaloyanov N, Toshkova R, Dimitrov G. Antitumour activity of novel 1,10-phenanthroline and 5-amino-1,10-phenanthroline derivatives. Eur J Med Chem. 2009;44(6):2720-2723, doi: 10.1016/j.ejmech.2009.01.036Get.
9. Georgieva A, Popov G, Shkondrov A, Toshkova R, Krasteva I, Kondeva-Burdina M, et al. Antiproliferate and antitumour activity of saponins from Astragalus glycyphyllos on myeloid *Graffi* tumour. J Ethnopharmacol. 2021;267;113519. doi: 10.1016/j.jep.2020.113519.
10. Minkova K, Toshkova R, Gardeva E, Tchorbadjieva M, Ivanova N, Yossifova L, et al. Antitumor activity of B-phycoerythrin from Porphyridium cruentum. J Pharm Res. 2011;4(5):1480-2.
11. Yakub G, Ignatova M, Manolova N, Rashkov I, Toshkova R, Georgieva A, et al. Chitosan/ferulic acid-coated poly(ε-caprolactone) electrospun materials with antioxidant, antibacterial and antitumor properties. Int J Biol Macromol. 2018;107A;680-702, doi: 10.1016/j.ijbiomac.2017.08.183.
12. Toshkova R, Ignatov I, Zvetkova R, Gluhchev G, Dinkov G. In vivo Effects of CortiNon+ on the Emergence and Progression of Experimental *Graffi* Tumor in Hamsters. Int Res J Oncol. 2020;3(1):27-36.
13. Toshkova R, Zvetkova E, Ignatov I, Gluhchev G. Effects of Catholyte water on the development of experimental *Graffi* tumor on hamsters. Bulg *J Public Health*. 2019;11(3):60-73.
14. Gramtikov P, Antonov A, Gramatikova M. A study of the properties and structure variations of water systems under the stimulus of outside influences. *Fresenius J Anal Chem.* 1992;343(1):134–5. doi10.1007/BF00332070.

15. Todorova L, Antonov A. Note on the drop evaporation method for study of water bond distribution I. An application to filtration *Comptes Rendus de l 'Academie* Bulg. des Sci. 2000;53(7):43-6.
16. Todorov S. Damianova A. Sivriev I. Antonov A. Galabova T. Water energy spectrum method and investigation of the variations of the H-bond structure of natural waters. *Comptes Rendus de l 'Academie* Bulg. des Sci. 2008;61(7):857–62.
17. Ignatov I, Huether F, Neshev N, Kiselova-Kaneva, Y, Popova TP, et al. Research of water molecules cluster structuring during *Haberlea rhodopensis* Friv. hydration. Plants. 2022;11(19):2655. doi:10.3390/plants11192655.
18. Ignatov I, Balabanski V, Angelcheva M. Application of infrared spectral analyses for medicinal plants containing calcium (Ca^{2+}). Plant Sci Today. 2022;9(4):1066–1073. doi: 10.14719/pst.1738.
18. Neshev N, Ignatov I, Drossinakis Ch. Measurement of hydrogen bond energies in some selected plants with medicinal properties and their information theoretical analysis. Plant Cell Biotechnol Mol Biol.2021;22 (45-46):79-94.
19. Ignatov I, Neshev N, Popova TP, Kiselova-Kaneva Y, Drossinakis Ch, Bankova R, et al. Theoretical analysis of hydrogen bonds energy distribution and information in a 1 % Rosa damascena Mill Oil Solution, Plant Sci. Today. 2022;9(3):760-5. doi10.14719/pst.1645.
20. Shannon CA. Mathematical theory of communication, *Bell Syst Tech.* J. 1948;27: 379–423, 623–656.
21. Meila M. Comparing clustering – An information based distance. *J Multivar Anal.* 2007;98:873-95. doi: 10.1016/j.jmva.2006.11.013Get.
22. Mehandjiev D, Ignatov I, Neshev N, Huether F, Gluhchev G, Drossiankis Ch. Formation of clusters in water and their distribution according to the number of water molecules. Bulg Chem Commun. 2022;54(3):211-216. doi: 10.34049/bcc.54.3.5489.
23. Sun X, Zhao Ch, Pan W, Wang J, Wang W. Carboxylate groups play a major role in antitumor activity of Ganoderma applanatum polysaccharide, carbohydrate polymers, Carbohydr Polym. 2015;123:283-7. doi: 10.1016/j.carbpol.2015.01.062.
24. Patil MP, Jin X, Simeon ChN, Palma J, Kim D, Ngabire D, et al. Anticancer activity of Sasa borealis leaf extract-mediated gold nanoparticles. Artif Cells Nanomed Biotechnol. 2018;46(1);82-8 doi: 10.1080/21691401.2017.1293675.
25. Hodnett EM, Dunn III W J. Cobalt Derivatives of schiff bases of aliphatic amines as antitumor agents. J Med Chem. 1972;15(3):339. doi: 10.1021/jm00273a037.
26. Moussa ZCh, El-sharief AM, Abbas SY. New imidazolidineiminothione derivatives: synthesis, spectral characterization and evaluation of antitumor, antiviral, antibacterial and antifungal activities. Eur J Med Chem. 2016;122:419-28. doi: 10.1016/j.ejmech.2016.06.051.
27. Ignatov I, Gluhchev G, Neshev N, Mehandjiev D. Structuring of water clusters depending on the energy of hydrogen bonds in electrochemically activated waters anolyte and catholyte, Bulg Chem Commun. 2021; 53(2):234-239. doi: 10.34049/bcc.53.2.5376.
28. Heine N, Fagiani MR, Rossi M, Wende T, Berden G, Blum V, et al. Isomer-selective detection of hydrogen-bond vibrations in the protonated water hexamer. J Am Chem Soc. 2013;135(22): 8266–73, doi: 10.1021/ja401359t.

Sažetak

RASPODJELA ENERGIJE VODIKOVIH VEZA I INFORMACIJSKO-TEORIJSKA ANALIZA KRVNOG SERUMA HRČKA S EKSPERIMENTALNIM GRAFFI TUMOROM

N. Neshev, I. Ignatov, R. Toshkova, C. Drossinakis, G. Gluhchev

Cilj ovog istraživanja bio je procijeniti mogućnost upotrebe raspodjele energije vodikovih veza (-E) i informacijsko-teorijskih karakteristika u krvnom serumu kao dijagnostičkih markera za tumorsku bolest na modelu hrčka s Graffi-jevim tumorom. Zlatni sirijski hrčci nasumično su podijeljeni u dvije skupine: zdravu kontrolnu i pokusnu skupinu s inokuliranim stanicama *Graffi-jevog* tumora. Raspodjela energija vodikovih veza (-E) u uzorcima krvnog seruma ispitivana je neravnotežnim procesom isparavanja kapljica i sekvencijalnim mjerenjem njihovog kuta vlaženja (Non-equilibrium Energy Spectrum (NES)). Prema dobivenim mjerenjima prosječna energija vodikove veze eksperimentalnih uzoraka bila je znatno niža od one kontrolnih. U eksperimentalnim uzorcima uočeni su pomaci u NES prema smanjenju energije vodikovih veza na razinama energije od 0,0937, 0,1187, 0,1212, 0,1337 i 0,1387 eV, te dodatna populacija na razinama energije od 0,0987, 0,1012, 0,1137 i 0,1237 eV u usporedbi s kontrolama. Za utvrđivanje mogućih razlika između eksperimentalnog i kontrolnog spektra korištene su informacijsko-teorijske mjere Shannonove entropije, Varijacije informacije i Transformacijske informacijske entropije. Iako su različite u svojim definicijama, nije pronađena statistički značajna razlika između tri informacijsko-teorijske mjere za eksperimentalne i kontrolne uzorke.

KLJUČNE RIJEČI: *vodikove veze, energija, informacija, entropija, krvni serum, tumor*